Structural and optical studies of laser ablated nanostructured CdTe thin films

M. NASIR KHAN[*], NASIR MAHMOOD[a], A. A. KHURRAM[b]
Physics Division, PINSTECH, P.O. Nilore, Islamabad - Pakistan
[a]Optics Laboratory, P.O. Nilore, Islamabad – Pakistan
[b]Experimental Physics Labs National Centre for Physics, Quaid-i-Azam University, Islamabad, 45320, Pakistan

Nanometer thin CdTe films were deposited on BK7 glass substrates using pulsed laser deposition technique in vacuum of 4.0×10^{-6} mbar. The as grown films were then annealed in air at different temperatures. These films were characterized by X-ray diffraction, optical and atomic force microscopy techniques for phase identification, structure and morphology. The optical properties of the films were measured using transmission and spectroscopic ellipsometry measurements. The chemical composition, thickness and interface of the substrate and films were studied by Rutherford backscattering spectroscopy. CdTe thin films prepared by this process are found to have single phase with cubic zinc blende structure. The growth occurred in the (111) preferential direction of the cubic structure. The optimized growth for crystalline and stoichiometric films possessing good structural and optical properties were achieved after annealing in air at 300°C. In the present study efforts have been made to correlate the optical properties of the CdTe thin films with the corresponding microstructural features associated with these films.

(Received August 10, 2012; accepted March 13, 2014)

Keywords: Photovoltaic, X-ray diffraction, CdTe thin films, Ellipsometry, RBS

1. Introduction

Nanometer thin film solar cells are an active area of research now a day. Different materials are being investigated for solar cell applications [1] leading to the development of new and innovative classes of semiconductor devices. Crystalline silicon, amorphous silicon and thin film polycrystalline materials like Cadmium Telluride (CdTe), Cadmium Zinc Telluride (CZT), Zinc Telluride (ZnTe) are prominent of these materials. Among the II–VI compounds, CdTe is the suitable material for the production of thin films solar cells due to its ideal band gap of 1.45 eV, high absorption coefficient, simple control for n-type or p-type conductivity, higher carrier mobility and ease in thin films fabrication. The choice of the material for solar cells depends upon the potential conversion efficiency expected from the devices made from these materials. CdTe is considered to be promising material due to its effective low cost, reliability for photovoltaics and high efficiency [2]. The growth and crystallization of CdTe nanocrystalline thin films are important because of their potential applications in semiconducting devices, photovoltaics, optoelectronic devices, radiation detectors, laser materials, thermoelectric devices, solar energy converters, solar cells, sensors and others audio -video nano-devices [3–6].

Recently polycrystalline CdTe materials were considered very suitable for the fabrication of solar cells because of their direct band gap. As a consequence of this direct energy gap, the absorption edge is very sharp and thus, more than 90% of the incident light is absorbed in few micron thickness of this material. The maximum photo current of 30.5 mA/cm^2 is measured for a CdTe cell corresponding to the standard global spectrum normalized to100 mW/cm^2. The maximum theoretical efficiency for this CdTe material is over 27%. Experimentally maximum energy conversion efficiency of 16.5% has been reported so for in CdTe thin films [7]. Cadmium telluride thin films can be fabricated by a variety of methods, such as vacuum deposition, electro-deposition, metal organic chemical vapor deposition (MOCVD), liquid phase epitaxy (LPE), molecular beam epitaxy (MBE), closed space sublimation (CSS) and screen printing etc. Among these methods vacuum deposition is an attractive method which has successfully been employed for the preparation of binary, inter metallic and ternary compounds. CdTe thin films would exhibit unusual charge carrier dynamics, improved collection of the photo-generated carriers and enhanced solar conversion efficiency because of the multiple reflections and the effective optical paths for absorption is much larger than the actual film thickness. The light generated electron and holes need to travel over a much shorter path and thus recombination losses are greatly reduced. As a result, the absorber layer thickness in nanostructured solar cells can be as thin as 150 nm instead of several micrometers in the traditional thin film solar cells [8]. Further, the energy band gap of various layers can be tailored to the desired design value by varying the size of nanoparticles. This allows for more design flexibility in the absorber and window layers in the solar cells [9]. Several researchers [10-16] have carried out research on preparation and characterization of CdTe thin films for photo- voltaic applications. In recent years,

efforts have been made to prepare nanocrystalline CdTe materials for various applications. However, the nanoparticles and nano thin films of CdTe materials are not well studied and only few papers are published [17-21]. Therefore, there is a lot of scope for studying these materials in nanometric scale. It is also well understood that the reduction in size (nanoparticles) will change the properties of these materials dramatically. Enormous amount of work has been carried out on structure, optical and electrical properties of CdTe thin films [22-25]. However it still requires further investigation to optimize low cost growth, structural, optical and electrical parameters of these nanocrystalline materials. In the present study, pulsed laser deposition technique has been used for the growth of CdTe nano films on low cost BK7 glass substrate by using bulk CdTe as the source material under high vacuum conditions. After optimizing the annealing parameters to obtain good quality nano structured thin films of this compound, their structural and optical properties have been studied in detail.

2. Experimental

Nanometer thin CdTe films were synthesized at room temperature by pulsed laser deposition technique. Nd: YAG Laser (Quantel) was used to ablate the CdTe target inside the chamber in vacuum maintained at 4.0×10^{-6} mbar. The glass substrate used was a soda lime glass (n =1.52 at 546 nm) supplied by Menzel, Germany. The pulsed laser deposition was performed with Nd: YAG laser at 1064 nm wavelength with average pulse energy 400 mJ/pulse, power density: 2.67×10^{9} W/cm^2, fluence 26.7 J/cm^2, pulse duration 10 ns, laser beam diameter 10 mm and 10 Hz repetition rate. The laser pulses were focused on the rotating CdTe disc target. CdTe target was a pre-sintered powder of CdTe pressed under the pressure of 6 tons in a circular disc with diameter 15mm and 5mm thickness. The incidence angle to the ablation target was 45°. The focused spot size on the target was about 1.5 mm^2. The distance between substrate and target was kept at 4 cm. The vacuum chamber was subsequently evacuated down to 4.0×10^{-6} mbar. No reactive gas was introduced in the chamber during deposition. The target and substrate holder during deposition were rotating in opposite directions with 4 and 6 rpm respectively. The deposition time was around 20 minutes. After deposition, annealing of the films was carried out in air at different temperatures of 200, 300, 400 and 500 ^{o}C for 2 hrs. The structure of these films was determined by X-ray diffraction using BrukerD8 diffractometer. The surface morphology was investigated through metallurgical optical microscope Olympus BX51 as well as atomic force microscope (E - AFM system). Transmission of the films was measured in the range 350 ~ 2500 nm using Perkin Elmer FTIR spectrum 2000. Absorption co-efficient (α), optical bandgap (E_g) were calculated from this data. The optical parameters of the film such as refractive index (n), extinction-co-efficient (k), real dielectric constant (ε_1) and imaginary dielectric constant (ε_2) were also calculated from the measured ellipsometric data in the range 400 ~750 nm by Ellipsometer (SE-850, SENTECH).

Rutherford Backscattering Spectroscopy (RBS) was carried out before and after the annealing to investigate the chemical compositions as well as the interface for interdiffusion between substrate and the films. The RBS spectra were taken using He^{++} beam from 5MV tandem pelletron accelerator at National Centre for Physics, Islamabad, Pakistan. The beam energy was 2MeV with beam current of 10 nA. All the spectra were taken at normal incidence. The simulation of the experimental RBS data was done by using SIMNRA version 6.05 (ion beam analysis software).

3. Results and discussion

3.1. Microstructural analysis

The θ-2θ XRD scans are shown in Fig. 1 for the as grown and that of the films annealed at different temperatures. The as grown films are amorphous as is evident from broad band in the X-ray diffraction pattern. In the annealing process, this broad band for the amorphous films changes to well defined sharp and strong reflection centered at an angle 2θ = 23.82^{o} indicating crystalline structure via the promotion of grains growth. The inhomogeneous stresses existing in the films during deposition process also reduce after the post deposition annealing. The best crystalline structure was obtained when annealed at 300 ^{o}C. The grain growth occurred along the (111) direction of the cubic structure. The crystalline film annealed at 300 ^{o}C possess cubic structure with a lattice constant of a = 6.464Å close to ASTM value of a_o = 6.481Å. The XRD results are well in agreement to the earlier studies by Dalchiele & Bonilla [26].

The grain size also increased with the annealing temperatures. The crystalline size was determined using Debye-Scherrer equation

$$D = \frac{K\lambda}{\beta \cos\theta} \tag{1}$$

where D is the crystallite size in the film, K is dimensionless constant (0.9). λ is the wavelength of X-ray, β is the full width at half-maximum (FWHM) of the diffraction peak and θ is the diffraction angle. The average crystallite size of film at 300 ^{o}C was 48 nm where it is 57 nm for the film annealed at 500 ^{o}C.

It was observed that annealing at higher temperatures > 300 ^{o}C, the peak shapes start deteriorating as is evident by the appearance of double edges (indicated by arrows) as well as re-broadening of the (111) diffraction peaks of the films annealed at 500 ^{o}C (Fig. 1). The phenomenon has been attributed to some sort of chemical reaction occurring between the CdTe films and substrate material resulting in partial crystallization of some additional phases at the interface.

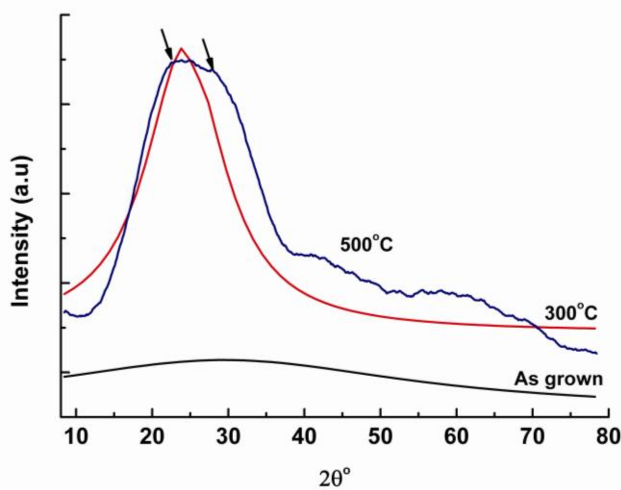

Fig. 1. θ -2θ scans for the as grown and annealed films.

Crystalline film surface morphology was assessed by optical and atomic force microscopes and is shown in Fig. 2(a-d). The optical micrograph for the as grown film showed dispersed Cd and Te amorphous phases with scratches and other defects visible Fig. 2 (a). On the other hand the film annealed at 300 ^{o}C on same magnification clearly shows the crystalline structure with grains uniformly distributed on the substrate surface Fig. 2 (b). AFM image of as grown film shown in Fig. 2 (c) revealed layer growth with nm thickness. The amorphous layer structure changed to the crystalline one when the film was annealed at 300 ^{o}C. The surface of the annealed film composed of small nanometer size grains and agglomerates as can be seen by small pyramidal islands in the AFM image [Fig. 2(d)] indicating the existence of barriers for grain boundary migration. The thermal energy supplied at this annealing temperature was enough to promote the reaction between the dispersed Cd and Te layers. Similar growth mechanism and growth in the (111) directional had earlier been reported for CdTe thin films [27-28].

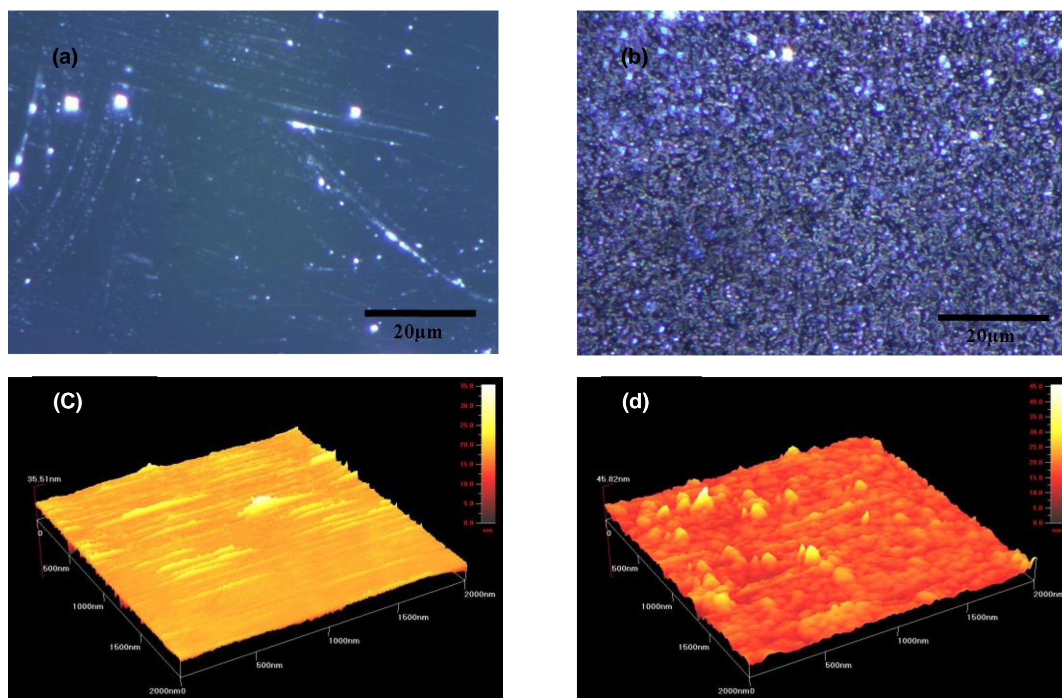

Fig. 2. Optical micrographs on same magnification (a) as grown (b) film annealed at 300 ^{o}C. (c-d): AFM images (c) as grown (d) film annealed at 300 ^{o}C.

3.2. Optical band gap determination

Transmission versus wavelength measurements for the as-deposited and that of annealed thin films at different temperatures are shown in Fig. 3. The experimentally measured transmission increases with increasing photon energy. More than 80 % of the transmission has been achieved in the measured wavelength range. The films annealed at 300 ^{o}C showed the characteristic absorption edge at 830 nm, whereas the as grown and the films annealed at 500 ^{o}C, lack such absorption edges. The tendency of the absorption edge to become more abrupt in 300 ^{o}C annealed films can be attributed to the observed improvement in the crystalline structure of the film.

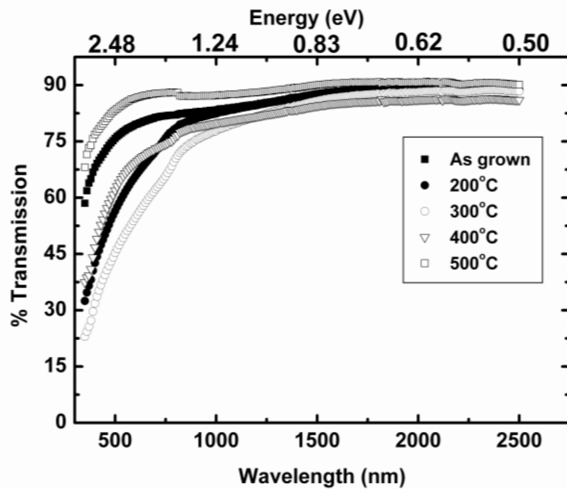

Fig. 3. Transmission versus wavelength for the as grown and that of films annealed at different temperatures.

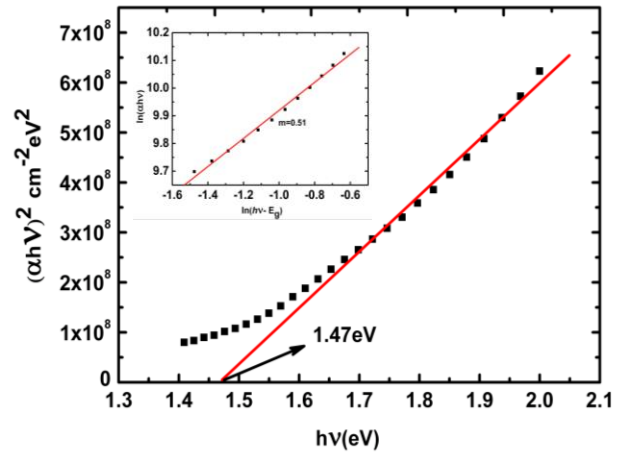

Fig. 4. Plot of $(\alpha h\nu)^2$ vs $h\nu$ in the band gap region and (inset) is the plot of $\ln(h\nu - E_g)$ vs. $\ln(\alpha h\nu)$ for the CdTe film annealed at 300 °C.

The data shown in Fig. 3 was used to determine the absorption coefficient, α, as a function of wavelength. The variation of $(\alpha h\nu)^2$ with energy ($h\nu$) for the film annealed at 300 °C is shown in Fig. 4. The band gap energy is obtained by intercepting the linear portion of the absorption curve to the energy axis. The band gap value of 1.47 eV obtained is independent of the annealing temperature and is in agreement with earlier findings for nanocomposites thin films as well as bulk CdTe at 300 K [29-31].

Generally in a compound semiconductor the absorption coefficient (α) is related to the incident photon energy ($h\nu$) via relation;

$$\alpha = (A/h\nu)\{h\nu - E_g\}^m \tag{2}$$

where A is constant, with value different for different transitions indicated by different values of m and E_g is the corresponding band gap. Using E_g value determined above the nature of optical transition (i.e., m value) was obtained from the plot of ln(α$h\nu$) vs. ln(h$\nu - E_g$) as shown in inset of Fig. 4. The value of m obtained for the films annealed at 300 °C comes out to be 0.51 which indicates a direct transition to be operative in these films. Thus, Equation (2) can be represented as;

$$\alpha = (A/h\nu)\{h\nu - E_g\}^{1/2} \tag{3}$$

The value of n = ½ has been reported earlier for CdTe nanocomposite thin film also exhibiting direct transitions [16].

3.3. Spectroscopic ellipsometry characterization

Spectroscopic ellipsometry was used to optically characterize the CdTe thin film annealed at 300 °C. Details about ellipsometry can be found in number of references [32-35]. In short, ellipsometry measures the changes in the state of polarization of light upon reflection from a surface. In general, reflection causes a change in the relative phase of p and s waves and in the ratio of their amplitudes. The effect of reflection is measured by two quantities, viz., Ψ (which measures the amplitude ratio) and Δ (which measures the relative phase change). An ellipsometric measurement allows one to quantify the phase difference between E_p and E_s, Δ, and the change in the ratio of their amplitudes given by tan Ψ. For a bare reflecting surface, the forms for Ψand Δ are:

$$\Delta = \delta_{r_p} - \delta_{r_s} \tag{4}$$

Where

$$\tan\Psi = \left|\frac{r_p}{r_s}\right| \tag{5}$$

If r_p and r_s be the reflection coefficients for the p and s components of the waves respectively, then their ratio (ρ) can be expressed as

$$\rho = \tan\Psi \exp(i\Delta) \tag{6}$$

The ellipsometry measurements directly generate the parameters of interest, Ψ and Δ. Fig. 5 shows the variations of Ψ and Δ with wavelength (λ) for the film annealed at 300 °C. The ellipsometric spectra were then fitted with an appropriate model assuming a realistic sample structure. For the film under study, the optical model used in the fitting of ellipsometric data consists of two layers on substrate. These two layers are native CdTe

layer on soda lime glass substrate and porous film layer on top. In this model, the unknown parameters, such as film thickness, optical constants, and constituent volume fractions are chosen as fitting parameters and are determined from standard ellipsometric equations as defined in reference [32].

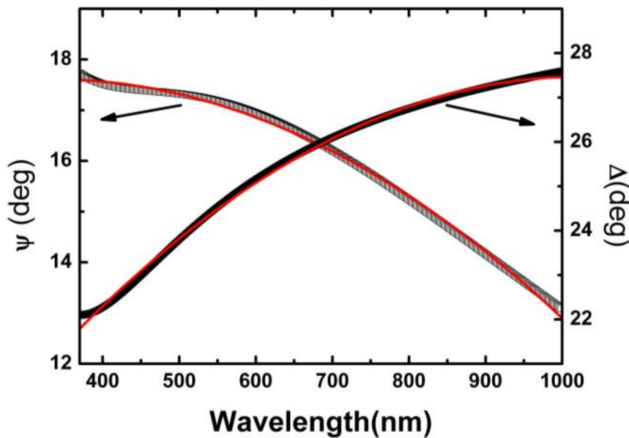

Fig. 5. Variation of Ψ and Δ with wavelength (λ) for CdTe film annealed at 300 °C.

Effective medium approximation (EMA) method was used to fit the data. EMA is the most frequently used approach to model the optical properties of thin films with two or more than two constituents. We have used Bruggeman EMA [35] and to simplify the data analysis, the optical constants such as refractive index of CdTe were directly taken from the database provided with the data analysis software of SENTECH 850 system. As mentioned above bilayer structure was considered for the data analysis. First native CdTe layer were taken on the BK7 glass substrate and the film thickness and the compositions were varied keeping the parameters of the dispersion relation of CdTe near the reference bulk values [36] and the best fit was obtained. Once the thickness and composition were determined to some extent, all other parameters were varied giving more weight to the variation of the optical constants. To further improve the fitting surface roughness was introduced as second layer. This was achieved by adding a surface layer of an effective medium of film materials and some percentage of voids (%CdTe + % voids) on the top of the film. This improved the fit to experimental data significantly as can be seen in Fig. 5. The volume fractions of the pores (or porosity) and thickness of the film along with other dispersion parameters were taken as fitting parameters. The film thickness comes out to be 46.02 nm with 11.2% voids. The de-polarization factor was 0.333 and MSE (mean square error) = 3 showing best fit to the experimental data (Fig. 5). Introduction of roughness layer requires careful handling of correlation of the fitted parameters so that it does not lead to physically irrelevant results. Correlation between fit parameters can be evaluated by cross correlation coefficients. The highest correlation coefficients found between the thickness of surface roughness layer and thickness of the thin film layer were found to be 0.24 indicating high sensitivity of the optical model to roughness induced changes in light polarization and is in fair agreement with results reported earlier [37].

The spectra of the real $\varepsilon_1(\omega)$ and imaginary $\varepsilon_2(\omega)$ part of the complex dielectric function $\varepsilon(\omega)$ along with measured refractive index (n) and extinction coefficient (k) data for 300 °C annealed film in the range 400-750 nm obtained from fitting of experimental ellipsometry data are shown in Fig. 6(a,b). The complex dielectric constant ($\varepsilon = \varepsilon_1 + i\varepsilon_2$) is fundamental intrinsic material property. The real part of which is associated with the term that describes how much it will slow down the speed of light in the material and is related to volume polarization for induced dipoles with increasing photon energy. The imaginary part on the other hand, describes how a dielectric absorb energy from electric field due to dipole motion (volume absorption term related to carriers generation). The imaginary part $\varepsilon_2(\omega)$ of the dielectric constant of the film depends on the absorption coefficient α and is related to valence to conduction band transitions having a close relation with band structure. Fig. 6(a) shows the variation of dielectric constants with photon energy for film annealed at 300 °C. It can be observed from the spectral dependences of ε, ε_1 and ε_2, that ε and ε_1 show a broad band in the measured wavelengths range. The ε_2 varies smoothly with photon energy revealing the absence of short range order in the film. The broad band for the ε and ε_1 in the measured wavelengths range can be attributed to crystalline nature with less porous character of the CdTe films. This is in agreement with the microstructural studies results mentioned above.

Fig. 6 (b) shows the variation of refractive index (n) and extinction coefficient (k) for the 300 °C annealed film obtained from the best fit of the experimental ellipsometry data. The refractive index (*n)* shows a strong spectral dependence reaching a peak value of ~3.15 in the vicinity of the band gap energy region before it tends to decrease sharply. The absorption decreases sharply in the film in the IR region. The extinction coefficient (k) also increases with increasing incident photon wavelength. Earlier it has been reported that in the case of glass substrate, the CdTe films have refractive index which is smaller than that of the monocrystalline CdTe and the phenomenon was attributed to the polycrystalline structure of the film [35, 38]. It was also reported earlier that refractive index of CdTe film on the monocrystalline Si substrate in the visible spectrum is 2.1, which is appreciably smaller than average value 2.5 of CdTe films grown on the CdHgTe substrate [31, 33]. This refractive index decrease was explained by the varied structure of the film and was

attributed to the lattice mismatch between Si and CdTe films. The refractive index value varies from 2.93 ~ 3.15 in the measured wavelength range for our 300 °C annealed film and is close to value of 3.13 reported earlier for bulk CdTe [39]. The increase in the extinction coefficient with wavelength can also be attributed to the increased crystallinity of the films with annealing. The values of the different optical constants determined for the 300°C annealed film are in close agreement with the earlier published data on CdTe nanocomposite films prepared by dc magnetron sputtering technique [16].

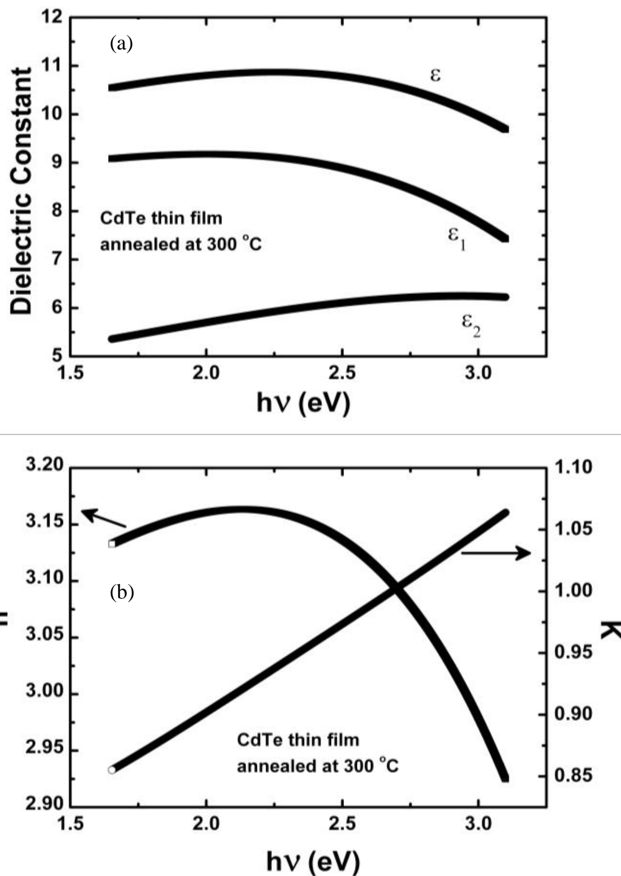

Fig. 6. Optical parameters derived from the spectroscopic ellipsometry data.

Fig. 7 shows the variation of optical conductivity with the incident photon energy. The optical conductivity is determined using the relation [40]

$$\sigma = \alpha\, n\, c / 4\pi \quad (7)$$

where *'c'* is the velocity of light. The optical conductivity directly depends on the absorption coefficient (α) and refractive index (n). The optical conductivity is found to increase sharply for higher energy values due to large absorption coefficient for these values.

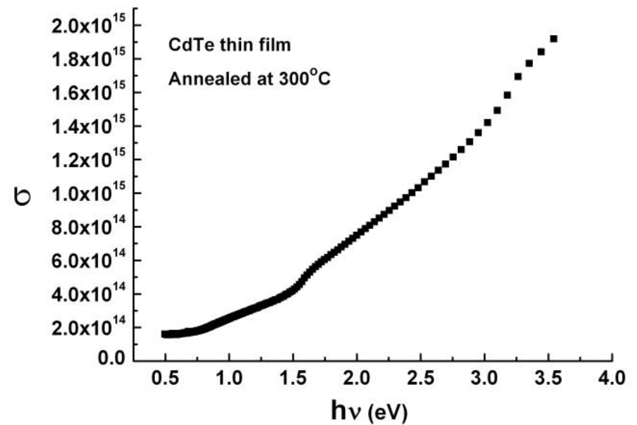

Fig. 7. Variation of optical conductivity with the incident photon energy.

3.5 RBS measurements

As mentioned above the XRD patterns of the as grown films have shown a broad band for the amorphous CdTe films, while those annealed at higher temperatures 500 °C showed double edges as well as re-broadening of the XRD peaks. The re-broadening and double edges observed in the 500 °C annealed films indicates that other phase formation is plausible as soda lime glass substrate used in this study contain both sodium and calcium as basic constituents. These elements possibly react with CdTe films at higher temperatures to form interfacial phases with different compositions. The XRD data along with microstructure studies by optical and AFM have unveiled that best crystallization of CdTe thin films can be achieved when annealed at 300 °C. These results also revealed that thermal energy supplied to the films when annealed at the temperature of 300 °C was enough to surpass the activation barrier for the reaction and to improve the crystallinity of films. In order to verify the above mentioned facts as well as stoichiometry of the films Rutherford backscattering spectroscopy of the as grown and that of annealed films was carried out. The RBS spectra used to study the interface diffusion and Cd/Te ratios of as-grown, 200, 300, 400 and 500°C samples are shown in Fig. 8. It can be seen from the shape of the RBS spectra that we have not observed any overlapping of the RBS signals for as-grown as well as those annealed at 200 and 300 °C. The sharp separation between the film and substrate spectra shows that there is negligible intermixing of film and substrate at the interface up to annealing temperature of 300 °C. However, as the annealing temperature has been increased to 400°C the RBS signals from the film and substrate started overlapping, the reason of the overlapping is the interdiffusion of the film and substrate material. The extent of the interdiffusion at the interface has been increased when the sample was further annealed at higher temperature of 500 °C. It was also observed from the simulation of the RBS data that the thickness of the CdTe

layer is not affected with the annealing up to 400°C, however, annealing at 500°C has decreased the thickness of the deposited CdTe layer to 25.4nm. The decrease in the film thickness is attributed to the diffusion of the Cd and Te into the substrate at higher annealing temperature. Moreover, the Cd to Te ratio has been decreased to 0.4 after 500 °C annealing showing greater diffusion of Cd into the substrate as compared to the Te. The parameters obtained after the simulation of the experimental data are given in Table 1.

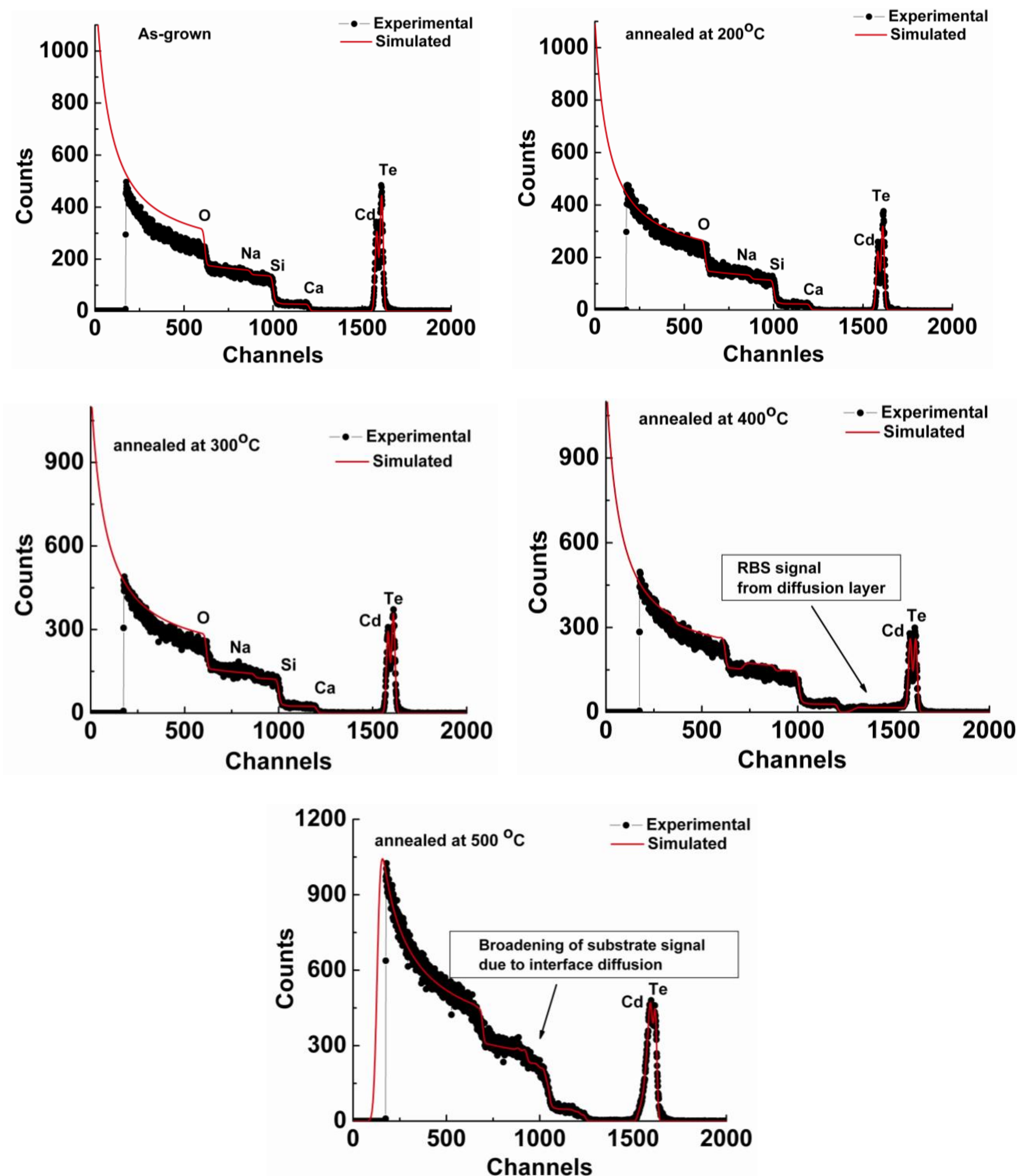

Fig. 8. Rutherford Backscattering Spectra of CdTe thin films (from top to bottom, as-grown, 200°C, 300°C, 400°C and 500°C annealed films); filled black circles experimental data, red line simulated spectra.

Table 1. Thin film parameters extracted from simulation of the RBS data.

Sample	Film Thickness (nm)	Cd %	Te%	Interdiffusion With substrate
As-grown	45.5	45	55	Nil
200°C annealed	45.9	45	55	Nil
300°C annealed	46.02	49	51	Nil
400°C annealed	45.9	53	47	Interface layer thickness 1400 nm cd= 0.001334 Te= 0.00135 Si= 0.238 O= 0.67 Ca= 0.028 Na= 0.06
500°C annealed	25.4	28	72	Huge overlap of substrate & film

4. Conclusion

CdTe films of nm thicknesses were successfully deposited on well cleaned soda lime glass substrates at room temperature by pulsed laser deposition technique. The analysis of the X-ray diffraction patterns showed that as deposited CdTe film exhibits amorphous structure changes to crystalline one when annealed at temperature of 300 °C. The annealed CdTe film possesses cubic zinc-blende structure with growth occurring on preferential (111) plane of the cubic structure. RBS analysis also confirmed that best crystallization of nanometer thick CdTe thin films with zero intermixing of the film and substrate is achieved after post-deposition annealing at 300 °C. AFM images showed nanocrystalline films with uniform morphology. Optical properties determined by optical transmittance and spectroscopic ellipsometry indicated direct allowed transition in the film similar to bulk crystalline semiconductors. The band gap calculated is 1.47 eV. The film thickness obtained through optical model fitting using ellipsometry data agrees well to the one obtained from RBS data simulation. The variations of several optical parameters such as refractive index, extinction coefficient and dielectric constant with photon energy obtained for the nanocrystalline film synthesized by laser ablation are found to be in fair agreement to the earlier findings for the nanocompsites CdTe films.

Acknowledgement

The authors thank Ms. B. Ilyas for assistance in the films growth. The help of Dr. M. Arshad Janjua in ellipsometry measurements is also highly appreciated.

References

[1] J. M. Kestner, S. McElvain, S. Kelly, T. R. Ohno, L. M. Woods, C. A. Wolden, Sol. Energy Mater. Sol. Cells **83**, 55 (2004).
[2] X. Duan, Y. Huang, R. Agarwal, C. M. Lieber, Nature **421**, 241 (2003).
[3] M Gratzel, .Nature **414**, 338 (2001).
[4] E. R Shaaban, N. Afify, A. El-Taher, J. Alloys & Compounds **482**, 400 (2009).
[5] L. Fang, L. Wu, Z. Lei, W. Li, Y. Cain,W. Cain, J. Zhang, Q. Lou, B. Li, J. Zhen, Thin Solid Films **515**, 5792 (2007).
[6] M. Burgelman, J. Verschraegen, S. Degrave, P. Nollet, Thin Solid Films **480-481**, 392 (2005).
[7] X. Wu, J. C. Keane, et al. in: Proceedings of the17th European photovoltaic Solar Energy Conference, Munich, Germany, Vol. II, 2001, pp.995.
[8] K. Ernst, A. Belaidi, R. Konenkamp, Semicond. Sci. & Technol. **18**, 475 (2003).
[9] R. S. Singh, V. K Rangari, S. Sanagapalli, V. Jayaraman, S. Mahendra, V. P. Singh, Solar Energy Materials and Solar Cells **82**, 315 (2004).
[10] S. Shanmugan, S. Balaji, D. Mutharasu, Mater. Lett. **63**, 1189 (2009).
[11] I. M. Dharmadasa, Curent Applied Physis **9**, 2 (2009).
[12] Jose Luis Cruz-Campa, David Zubia, Solar Energy Materials and Solar Cells **93**, 15 (2009).
[13] N. Armani, G. Salviati, L. Nasi, A. Bosio, S. Mazzamuto, N. Romeo, Thin Solid Films **515**, 6184 (2007).
[14] A. Boise, N. Romeo, S. Mazzamuto,VittorioCanevari, Progr. Cryst. Growth Character. Mater. **52**, 247 (2006).
[15] T. Shiga, K. Takechi, T. Motohiro, .Solar Energy Materials and Solar Cells **90**, 1849 (2006).
[16] S. K. Bera, D. Bhattacharyya, R. Ghosh, G. K. Paul, Appl. Surf. Sci. **255**, 6634 (2009).

[17] N. Romčević, M. Romčević, R. Kostić, D. Stojanović, G. Karczewski, R. Galazka. Microelectronics Journal **40**, 830 (2009).
[18] L. Hu, Z. Mao, C. Gao, Colloids and Surfaces A **336**, 115 (2009).
[19] J. Li, G. Zou, X. Hu, X. Zhang., J. Electroanal. Chem. **625**, 88 (2009).
[20] S. A. Khan, A. A. Al-Ghamdi, Mater. Lett. **63**, 1740 (2009).
[21] A. A. Al-Ghamdi, S. A. Khan, Physica B **404**, 4262 (2009).
[22] S. Singh, R. Kumar, K. N. Sood, Thin Solid Films **519**, 1078 (2010).
[23] A. A. Al-Ghamdi, S. A. Khan, A. Nagat, M. S.AbdEl-Sadek, Optics & Laser Technology **42**, 1181 (2010).
[24] N. EL-Kadry, A. Ashour, S. A. Mahmoud, Thin Solid Films **269**, 112 (1995).
[25] Joel, Pantoja Enrquez, Xavier Mathew, J. Cryst. Growth **259**, 215 (2003).
[26] E. A. Dalchiele, S. Bonilla, J. Braz. Chem. Soc. **3**, 95 (1992).
[27] M. Bayhan, Tr. J. Phys. **22**, 929 (1998).
[28] E. Saucedo, V. Corregidor, L. Fornaro, A. Cuna, E. Dieguez, Thin Solid Films **471**, 304 (2005).
[29] S. Jimenez-Sandoval, M. Melediz –Lira, I. Hernandez-Calderon, J. Appl. Phys. **72**, 4197 (1992).
[30] R. W. Miles, M. T. Bhatti, K. M. Hynes, A. E. Baumann, R. Hill, Mater. Sci. & Engg. B **16**, 250 (1993).
[31] P. M. Amirtharaje, F. H. Pollak, J. R. Waterman, P. R. Boyd, Appl. Phys. Lett. **41**, 860 (1982).
[32] R. M. A. Azzam, N. M. Bashara, In: Ellipsometry and Polarized Light. Amsterdam: North-Holland Publishing Co. 1977.
[33] P. G. Snyder, J. A. Woollam, S. A. Alterovitz, B. D. Johs, J. Appl. Phys. **68**, 5925 (1990).
[34] D. E. Aspnes, J. B. Theeten, Phys. Rev. B **20**, 288 (1979).
[35] D. A. G. Bruggeman, Ann. Phys. (Leipzig) **24**, 636 (1935).
[36] P. Lautenschlager, S. Logothetidis, L. Via, M. Cardona, Phys. Rev. B **32**, 3811 (1985).
[37] G. E. Jellison Jr., Thin Solid Films **234**, 416 (1993).
[38] J. Ramiro, A. Perea, J. F. Trigo, Y. Laaziz, E. G. Camarero, Thin Solid Films **361-362**, 65 (2000).
[39] K. N. Kornienko, V. A. Odarych, L. V. Poperenko, M. V. Vuichik, Func. Mater. **13**, 179 (2006).
[40] J. I. Pankove, "Optical Processes in Semiconductors" Dover Publications, Inc. New York, 1971, p-91.

*Corresponding author: nasir852001@yahoo.com; nasir85@hotmail.com; nasir@pinstech.org.pk